Publication IV

Piippo, A. and Luomi, J. (2006). "Inductance harmonics in permanent magnet synchronous motors and reduction of their effects in sensorless control." In *Proceedings of the XVII International Conference on Electric Machines (ICEM 2006)*, no. 138, Chania, Greece, CD-ROM.

Inductance Harmonics in Permanent Magnet Synchronous Motors and Reduction of Their Effects in Sensorless Control

Antti Piippo and Jorma Luomi

***Abstract*—The paper deals with speed and position estimation of permanent magnet synchronous motors having unwanted spatial harmonics in the stator inductance and in the permanent magnet flux. The sensorless control is based on an adaptive observer that is augmented with a pulsating high-frequency signal injection technique at low speeds. The effects of harmonics on the speed and position estimation are reduced by adding harmonic models of the inductances and the flux to the adaptive observer and by modifying the injected high-frequency voltage signal based on the inductance variation. Simulations and laboratory experiments show that the estimation accuracy is improved and torque pulsations are reduced.**

***Index Terms*—Permanent magnet synchronous motors, sensorless control, signal injection, spatial harmonics.**

I. Introduction

INFORMATION on the rotor position is required for the vector control of a permanent magnet synchronous motor (PMSM). In sensorless control, the rotor speed and position are obtained by means of a suitable estimation algorithm. These estimation algorithms can be classified into fundamental-excitation methods [1]–[3] and signal injection methods [4]–[6]. The former, based on the back-emf of the motor, have good dynamic properties, whereas the latter, based on detecting magnetic anisotropy, are suited for estimation at low speeds. To combine the advantages of the two approaches, the estimation method can be changed from a fundamental-excitation method to either a high-frequency (HF) signal injection method [7], [8] or a combined method [9], [10] at low speeds.

In permanent magnet synchronous machines, unidealities in the rotor geometry and in the magnetomotive force distribution result in a non-sinusoidal variation of the back-emf and in spatial harmonics in the stator inductances [11]. These unidealities not only cause ripple in the electromagnetic torque [12], but also lead to errors in the rotor speed and position estimation. The effects of inductance harmonics have earlier been modeled in rotating HF signal injection methods for induction machines [13]–[15].

The aim of this paper is to increase the accuracy of the rotor speed and position estimation of PMSMs when the spatial variation of the stator inductances and flux linkages is non-sinusoidal. An adaptive observer is used throughout the whole speed region, and it is augmented with a pulsating HF signal injection method at low speeds [10]. The adaptive observer is extended with a model for the inductance and flux harmonics, and the HF voltage reference of the signal injection method is modified for compensating the estimation error caused by the inductance harmonics. The performance of the method is investigated by means of simulations and experiments.

II. Permanent Magnet Motor Model

The PMSM is modeled in the *d-q* reference frame fixed to the rotor. The *d* axis is oriented along the permanent magnet flux, whose angle in the stator reference frame is θ_m in electrical radians. The stator voltage equation is

$$\mathbf{u}_s = R_s \mathbf{i}_s + \dot{\boldsymbol{\psi}}_s + \omega_m \mathbf{J} \boldsymbol{\psi}_s \tag{1}$$

where $\mathbf{u}_s = [u_d \quad u_q]^T$ is the stator voltage, $\mathbf{i}_s = [i_d \quad i_q]^T$ the stator current, $\boldsymbol{\psi}_s = [\psi_d \quad \psi_q]^T$ the stator flux, R_s the stator resistance, ω_m the electrical angular speed of the rotor, and

$$\mathbf{J} = \begin{bmatrix} 0 & -1 \\ 1 & 0 \end{bmatrix}$$

The stator flux is

$$\boldsymbol{\psi}_s = \mathbf{L} \mathbf{i}_s + \boldsymbol{\psi}_{pm} \tag{2}$$

where $\mathbf{L}$ is the inductance matrix and $\boldsymbol{\psi}_{pm}$ is the permanent magnet flux.

When the rotor position angle θ_m is varied, the permanent magnet flux linkages of the three stator winding phases consist of a fundamental component and odd harmonics. In the *d-q* reference frame, the permanent magnet flux has a constant component ψ_{pm0} on the *d* axis and harmonics of orders multiple of six. For simplicity, the harmonics having orders higher than six are omitted in this paper, resulting in the permanent magnet flux vector [11]

$$\boldsymbol{\psi}_{pm} = \begin{bmatrix} \psi_{pm0} + \psi_{d6} \cos(6\theta_m) \\ \psi_{q6} \sin(6\theta_m) \end{bmatrix} \tag{3}$$

Manuscript received June 30, 2006. This work was financially supported by ABB Oy and Walter Ahlström Foundation.

The authors are with the Power Electronics Laboratory, Helsinki University of Technology, P.O. Box 3000, FI-02015 TKK, Finland (phone: +358-9-451 5955; fax: +358-9-451 2432; e-mail: antti.piippo@tkk.fi).

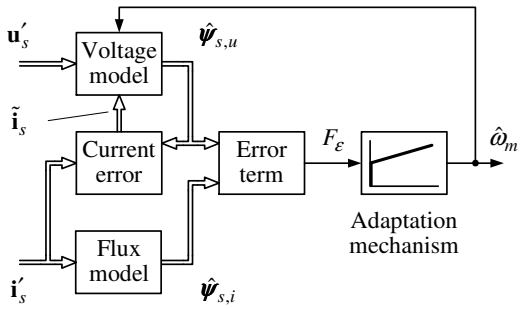

Fig. 1. Block diagram of the adaptive observer.

where ψ_{d6} and ψ_{q6} are the coefficients of the sixth-order harmonics on the *d* and *q* axes, respectively.

The self and mutual inductances of the stator winding phases have an average component and even harmonics when the rotor position angle is varied. In the *d-q* reference frame, the inductance matrix consists of the direct-axis inductance L_d and quadrature-axis inductance L_q on the *d* and *q* axes, respectively, and harmonics of orders multiple of six. When the higher-order harmonics are omitted, the stator inductance matrix is [11], [16]

$$\mathbf{L} = \begin{bmatrix} L_d + L_6\cos(6\theta_m) & -L_6\sin(6\theta_m) \\ -L_6\sin(6\theta_m) & L_q - L_6\cos(6\theta_m) \end{bmatrix} \tag{4}$$

where L_6 is the amplitude of the sixth harmonic of the stator inductance.

The electromagnetic torque is given by

$$\begin{aligned} T_e = \frac{3p}{2}\big[&\psi_{pm0} i_q + (L_d - L_q) i_d i_q \\ &-2L_6\sin(6\theta_m)(i_d^2 - i_q^2) \\ &-4L_6\cos(6\theta_m) i_d i_q \\ &+i_q\cos(6\theta_m)(\psi_{d6} + 6\psi_{q6}) \\ &-i_d\sin(6\theta_m)(\psi_{q6} + 6\psi_{d6})\big] \end{aligned} \tag{5}$$

where *p* is the number of pole pairs.

III. Observer Structure

A. Adaptive Observer

In the adaptive observer, the rotor speed and position estimation is based on the estimation error between two different models (a reference model and an adaptive model). In the following, the stator flux is the estimated variable, and the estimate of the rotor speed is used for adjusting the adaptive model [10].

The block diagram of the adaptive observer is shown in Fig. 1. The observer is formulated in the estimated rotor reference frame. The reference model is based on (2); this flux model can be written as

$$\hat{\boldsymbol{\psi}}_{s,i} = \hat{\mathbf{L}}\mathbf{i}_s' + \hat{\boldsymbol{\psi}}_{pm} \tag{6}$$

Estimated quantities are marked by ˆ and measured quantities expressed in the estimated rotor reference frame are marked by ´. Originally, the stator inductance matrix is a diagonal matrix with the diagonal elements L_d and L_q, and the permanent magnet flux has only the constant component ψ_{pm0}. They can be extended to include the harmonics using the definitions (3) and (4).

The adaptive model is based on (1) and (2). It is here referred to as a voltage model, and defined by

$$\dot{\hat{\boldsymbol{\psi}}}_{s,u} = \mathbf{u}_s' - \hat{R}_s\hat{\mathbf{i}}_s - \hat{\omega}_m\mathbf{J}\hat{\boldsymbol{\psi}}_{s,u} + \boldsymbol{\lambda}\tilde{\mathbf{i}}_s \tag{7}$$

where the estimate of the stator current and the estimation error of the stator current are

$$\hat{\mathbf{i}}_s = \hat{\mathbf{L}}^{-1}(\hat{\boldsymbol{\psi}}_{s,u} - \hat{\boldsymbol{\psi}}_{pm}) \tag{8}$$

$$\tilde{\mathbf{i}}_s = \mathbf{i}_s' - \hat{\mathbf{i}}_s \tag{9}$$

respectively. The feedback gain matrix $\boldsymbol{\lambda}$ is varied as a function of the rotor speed [17].

For the adaptation, an error term is constructed as

$$F_\varepsilon = \mathbf{C}_1\tilde{\boldsymbol{\psi}}_s \tag{10}$$

where $\tilde{\boldsymbol{\psi}}_s = \hat{\boldsymbol{\psi}}_{s,i} - \hat{\boldsymbol{\psi}}_{s,u}$ is the difference between the flux estimates, and $\mathbf{C}_1 = \begin{bmatrix} 0 & 1 \end{bmatrix}$. Hence the flux difference in the estimated *q* direction is used. The estimate of the electrical angular speed of the rotor, used in (7), is obtained by a PI speed adaptation mechanism

$$\hat{\omega}_m = -k_p F_\varepsilon - k_i\int F_\varepsilon dt \tag{11}$$

where k_p and k_i are nonnegative gains. The estimate for the rotor position is evaluated by integrating $\hat{\omega}_m$. The gains k_p and k_i of the adaptation mechanism are selected as [10]

$$k_p = \frac{2\alpha_{fo}}{\hat{\psi}_{pm0}}, \quad k_i = \frac{\alpha_{fo}^2}{\hat{\psi}_{pm0}} \tag{12}$$

where the design parameter α_{fo} corresponds to the approximate bandwidth of the adaptive observer.

B. Coupling HF Signal Injection to the Adaptive Observer

Since the adaptive observer cannot perform well at low speeds due to inaccuracies in measurements and parameter estimates, an HF signal injection method is used to stabilize the observer [10]. A carrier excitation signal alternating at angular frequency ω_c and having amplitude u_c is superimposed on the *d* component of the stator voltage in the estimated rotor reference frame. The injected HF voltage signal is thus

$$\mathbf{u}_c = u_c\cos(\omega_c t)\begin{bmatrix} 1 \\ 0 \end{bmatrix} \tag{13}$$

An alternating HF current response is detected in the *q* direction. Demodulation and low-pass filtering results in an error signal $\varepsilon \approx 2K_\varepsilon\tilde{\theta}_m$, which is approximately proportional to the position estimation error $\tilde{\theta}_m = \theta_m - \hat{\theta}_m$, K_ε being the signal injection gain.

The error signal ε is used for correcting the estimated rotor speed and position by influencing the direction of the stator

flux estimate of the adaptive model. The algorithm is given by

$$\dot{\hat{\boldsymbol{\psi}}}_{s,u} = \mathbf{u}'_s - \hat{R}_s \hat{\mathbf{i}}_s - (\hat{\omega}_m - \omega_\varepsilon)\mathbf{J}\hat{\boldsymbol{\psi}}_{s,u} + \boldsymbol{\lambda}\tilde{\mathbf{i}}_s \tag{14}$$

and

$$\omega_\varepsilon = \gamma_p \varepsilon + \gamma_i \int \varepsilon dt \tag{15}$$

where γ_p and γ_i are the gains of the PI mechanism driving the error signal ε to zero. In accordance with [9], these gains are selected as

$$\gamma_p = \frac{\alpha_i}{2K_\varepsilon}, \quad \gamma_i = \frac{\alpha_i^2}{6K_\varepsilon} \tag{16}$$

where α_i is the approximate bandwidth of the PI mechanism.

At low speeds, the combined observer relies both on the signal injection method and on the adaptive observer. The influence of the HF signal injection is decreased linearly with increasing speed, reaching zero at transition speed ω_Δ [10]. At higher speeds, the estimation is based only on the adaptive observer.

IV. Modification of the Signal Injection Method

A. Position Error Caused by Inductance Harmonics

For the HF signal injection method, it is possible to solve the position estimation error caused by stator inductance harmonics. The motor model is expressed in terms of the stator current by substituting (2) for the stator flux in the voltage equation (1):

$$\mathbf{u}_s = R_s \mathbf{i}_s + \mathbf{L}\dot{\mathbf{i}}_s + \dot{\mathbf{L}}\mathbf{i}_s + \dot{\boldsymbol{\psi}}_{pm} + \omega_m \mathbf{J}\mathbf{L}\mathbf{i}_s + \omega_m \mathbf{J}\boldsymbol{\psi}_{pm} \tag{17}$$

The PMSM model is then transformed to the estimated rotor reference frame. The resulting stator current derivative in the estimated rotor reference frame is derived in the Appendix.

Since the HF signal injection method is applied only at low speeds, the approximation $\omega_m = 0$ is used. The resistive voltage drop is also omitted when the HF signal injection is considered. The permanent magnet flux derivative is proportional to the rotor speed, and is thus also omitted when ω_m is low. The current derivative is simplified to

$$\dot{\mathbf{i}}'_s = (\mathbf{L}^{-1} - \tilde{\theta}_m \mathbf{L}^{-1}\mathbf{J} + \tilde{\theta}_m \mathbf{J}\mathbf{L}^{-1})\mathbf{u}'_s \tag{18}$$

When the HF voltage signal (13) is fed to the stator winding, the derivative of the q-axis current is obtained from (18). If the rotor position and the position error are considered constant, the q-axis current can be solved by integration. When the sixth inductance harmonic is included in the stator inductance matrix as in (4), the resulting q-axis current is given by (19) below.

The q-axis HF current is demodulated, low-pass filtered, and driven to zero in steady state. Hence the rational expression in (19) becomes zero. Setting the numerator of (19) equal to zero yields the rotor position error

$$\tilde{\theta}_m = \frac{-L_6 \sin(6\theta_m)}{(L_q - L_d) - 2L_6 \cos(6\theta_m)} \tag{20}$$

The inductance harmonic thus causes a periodic error in the rotor position estimate when the original HF signal injection method is used for the estimation.

B. Error Compensation

The position error caused by inductance harmonics can be compensated by modifying the HF voltage signal (13). It is required that at the zero rotor position error, the signal injection method receives the HF current signal

$$\mathbf{i}_s = \frac{u_c}{L_d \omega_c} \sin(\omega_c t) \begin{bmatrix} 1 \\ 0 \end{bmatrix} \tag{21}$$

Inserting this current into (17) gives the HF voltage signal to be fed to the motor. The resistive voltage drop and the back-emf are ignored. The resulting modified HF voltage signal is

$$\begin{aligned} \mathbf{u}_c = {} & u_c \cos(\omega_c t) \begin{bmatrix} 1 + (L_6 / L_d)\cos(6\theta_m) \\ -(L_6 / L_d)\sin(6\theta_m) \end{bmatrix} \\ & + \frac{\omega_m}{\omega_c} u_c \sin(\omega_c t) \begin{bmatrix} -5(L_6 / L_d)\sin(6\theta_m) \\ 1 - 5(L_6 / L_d)\cos(6\theta_m) \end{bmatrix} \end{aligned} \tag{22}$$

Thus the HF voltage should be augmented with a signal whose amplitude is a function of the rotor position and proportional to the amplitude L_6 of the harmonic inductance in order to obtain a more accurate position estimate. An HF voltage signal is superimposed on the q component of the stator voltage in addition to the d component in the estimated rotor reference frame.

V. Results

The proposed method was investigated by means of simulations and laboratory experiments. The block diagram of the control system comprising cascaded speed and current control loops is shown in Fig. 2. PI-type speed control with active damping is used. The current component references $i_{d,ref}$ and $i_{q,ref}$ are calculated according to maximum torque per current control [18]. The current control is implemented as PI-type control in the estimated rotor reference frame, where the cross-coupling terms and the back-emf are decoupled [19]. The dc-link voltage of the converter is measured, and a simple current feedforward compensation for dead times and power device voltage drops is applied [20].

The experimental setup is illustrated in Fig. 3. A six-pole interior-magnet PMSM (2.2 kW, 1500 rpm) is fed by a frequency converter that is controlled by a dSPACE DS1103 PPC/DSP board. The motor data are given in Table I. Me-

$$i'_q = \frac{L_6 \sin(6\theta_m) + \tilde{\theta}_m (L_q - L_d) - 2L_6 \tilde{\theta}_m \cos(6\theta_m)}{L_d L_q + L_6 \cos(6\theta_m)(L_q - L_d) - L_6^2} \frac{u_c}{\omega_c} \sin(\omega_c t) \tag{19}$$

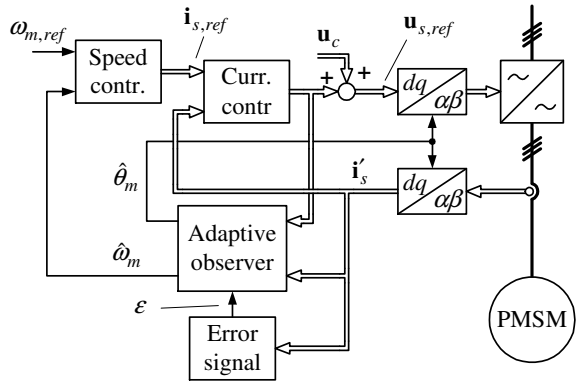

Fig. 2. Block diagram of the control system. Block "Speed contr." includes both the speed controller and the minimization of the current amplitude.

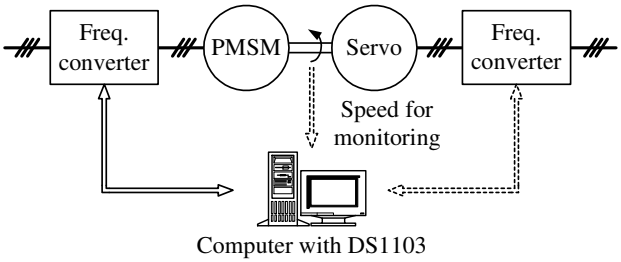

Fig. 3. Experimental setup. Mechanical load is provided by a servo drive.

chanical load is provided by a PMSM servo drive. An incremental encoder is used for monitoring the actual rotor speed and position. The nominal dc-link voltage is 540 V, and the switching frequency and the sampling frequency are both 5 kHz. The HF carrier excitation signal has a frequency of 833 Hz and a zero-speed amplitude of 40 V, and the amplitude becomes zero at the transition speed ω_Δ = 0.13 p.u. The electromagnetic torque is limited to 22 Nm, which is 1.57 times the nominal torque T_N. Other parameters of the control system are given in Table II.

The MATLAB/Simulink environment was used for the simulations. Fig. 4 shows the rotor position error as a function of the rotor position at no-load in steady state. The rotor speed reference was as low as 0.0015 p.u in the simulations. The simulation result obtained using the original HF voltage signal (13) corresponds well to the error evaluated analytically using (20). When the modified HF voltage signal (22) is used, the estimation error is reduced significantly.

Although the frequency of the HF voltage signal is above the current controller bandwidth of 400 Hz, the current control tries to compensate the HF current. To reduce this compensation, the estimated current is used for feedback in the proportional part of the current controller instead of the measured current. However, the current controller causes a small periodic error in the estimated position, which can be seen in Fig. 4. Almost zero error could be achieved by filtering the current or the fundamental voltage reference, but the filtering would degrade the current control performance.

Fig. 5 shows experimental results at the nominal load torque and constant speed in the motoring mode. Only the adaptive

TABLE I
MOTOR DATA

Nominal power	2.2 kW
Nominal voltage	370 V
Nominal current	4.3 A
Nominal frequency	75 Hz
Nominal speed	1 500 rpm
Nominal torque T_N	14 Nm
Number of pole pairs p	3
Stator resistance R_s	3.59 Ω
Direct-axis inductance L_d	36 mH
Quadrature-axis inductance L_q	51 mH
Inductance harmonic amplitude L_6	1.1 mH
Permanent magnet flux ψ_{pm0}	0.545 Vs
Flux harmonic coefficient ψ_{d6}	−1.0 mVs
Flux harmonic coefficient ψ_{q6}	1.4 mVs
Total moment of inertia	0.015 kgm^2

TABLE II
CONTROL SYSTEM PARAMETERS

Current controller bandwidth	2π 400 rad/s
Speed controller bandwidth	2π 5 rad/s
Speed adaptation bandwidth α_{fo}	2π 50 rad/s
Bandwidth α_i at zero speed	2π 5 rad/s

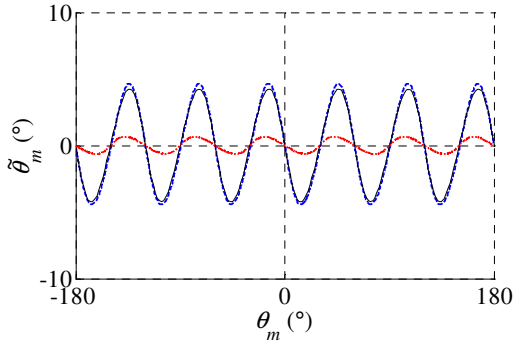

Fig. 4. Rotor position estimation error as a function of the rotor position: analytical (solid), simulated with original HF voltage signal (dashed), and simulated with modified HF voltage signal (dotted).

observer contributes to the speed estimation at the speed ω_m = 0.2 p.u. Results obtained without and with the sixth harmonics in the flux vector (3) and in the inductance matrix (4) are depicted. The speed variation at the sixth harmonic of the stator frequency is reduced significantly when the model for the inductance and flux variation is added to the observer. It is to be noted that electromagnetic torque harmonics exist even without any position error.

Experimental results showing speed reference steps at low speeds are shown in Fig. 6. The HF signal injection is in use at the speed 0.02 p.u. When the model for the harmonics is not used, pulsation at the sixth harmonic of the stator frequency can be seen in the rotor speed and its estimate. When the sixth harmonic is added to the inductance and flux models and the modified HF voltage signal is used, the speed pulsation is reduced and the position estimation accuracy is improved. Al-

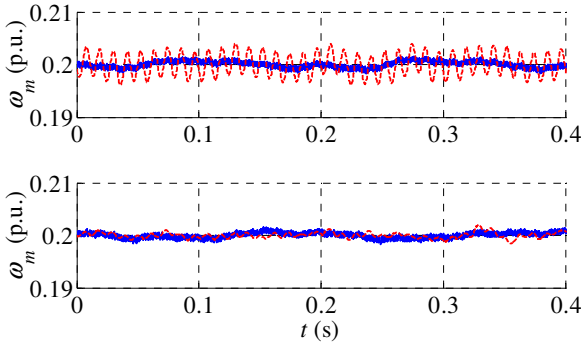

Fig. 5. Experimental results at nominal load torque and constant speed operation: electrical angular speed (solid), its estimate (dashed), and its reference (dotted). First subplot shows the operation without models for inductance and flux variation, and second subplot shows operation with models for inductance and flux variation.

though the pulsation at the sixth harmonic is reduced, errors at other frequencies are still present, for example, due to current measurement inaccuracies.

Fig. 7 depicts experimental results of a slow speed reversal at the nominal load torque. The position estimation accuracy at low speeds is improved due to the modified HF voltage signal, and the pulsation of the speed estimate is reduced.

VI. Conclusion

The rotor speed and position of a PMSM can be estimated in a wide speed range by means of an adaptive observer that is augmented with an HF signal injection technique at low speeds. The effects of inductance and flux harmonics on the speed an position estimation can be reduced by simple modifications in the algorithm. Models for the spatial harmonics are added to the stator inductance and the permanent magnet flux, and a position-dependent component is added to the injected HF voltage signal. In the examples given in the paper, the sixth harmonic of the inductance and the flux are taken into account and, consequently, the sixth harmonics in the estimation error, torque and speed are reduced.

Appendix

The stator voltage and current transformed from the true rotor reference frame into the estimated rotor reference frame are

$$\mathbf{u}_s' = \mathbf{T}\mathbf{u}_s \tag{23a}$$

$$\mathbf{i}_s' = \mathbf{T}\mathbf{i}_s \tag{23b}$$

respectively, where $\mathbf{T} = \cos(\tilde{\theta}_m)\mathbf{I} + \sin(\tilde{\theta}_m)\mathbf{J}$ is the coordinate transformation matrix. The vectors $\mathbf{u}_s$ and $\mathbf{i}_s$ are solved from (23) and substituted in (17). Solving the stator voltage in the estimated rotor reference frame gives

$$\begin{aligned}\mathbf{u}_s' = R_s\mathbf{i}_s' + \mathbf{T}\mathbf{L}\frac{d}{dt}(\mathbf{T}^{-1}\mathbf{i}_s') + \mathbf{T}\dot{\mathbf{L}}\mathbf{T}^{-1}\mathbf{i}_s' \\ +\mathbf{T}\boldsymbol{\psi}_{pm} + \omega_m\mathbf{T}\mathbf{J}\mathbf{L}\mathbf{T}^{-1}\mathbf{i}_s' + \omega_m\mathbf{T}\mathbf{J}\boldsymbol{\psi}_{pm}\end{aligned} \tag{24}$$

After applying the product rule for differentiation and differentiating $\mathbf{T}$, the current derivative can be solved. The derivative of the stator inductance matrix is

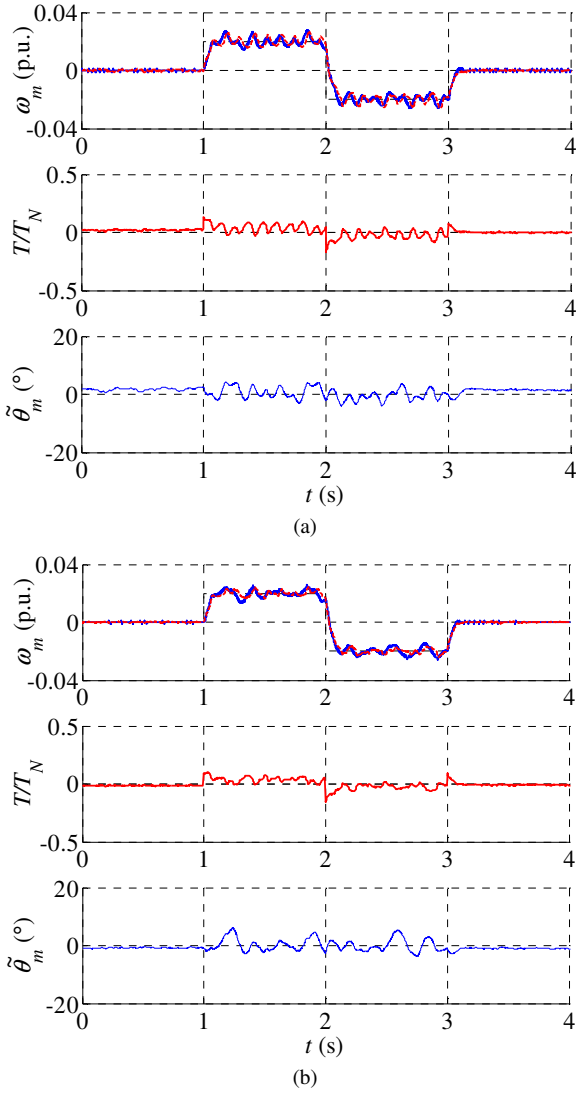

Fig. 6. Experimental results showing speed reference steps at zero load torque: (a) original HF voltage signal and no models for inductance and flux variation; (b) modified HF voltage signal and models for inductance and flux variation. First subplot shows electrical angular speed (solid), its estimate (dashed), and its reference (dotted). Second subplot shows estimated electromagnetic torque (solid) and load torque reference (dotted). Last subplot shows estimation error of rotor position in electrical degrees.

$$\dot{\mathbf{L}} = -6\omega_m\mathbf{J}\mathbf{L}_h \tag{25}$$

where the sixth-harmonic contribution to the stator inductance matrix is

$$\mathbf{L}_h = L_6\begin{bmatrix}\cos(6\theta_m) & -\sin(6\theta_m) \\ -\sin(6\theta_m) & -\cos(6\theta_m)\end{bmatrix} \tag{26}$$

When the rotor position error is assumed small and hence $\cos(\tilde{\theta}_m) \approx 1$, $\sin(\tilde{\theta}_m) \approx \tilde{\theta}_m$, and $\tilde{\theta}_m^2 \approx 0$, the current derivative in the estimated rotor reference frame is:

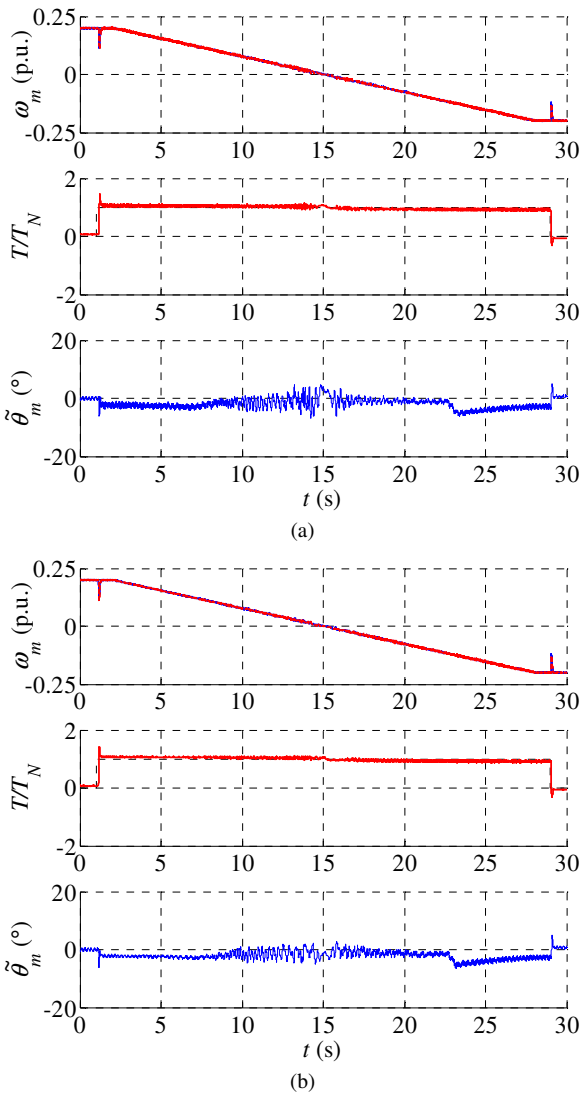

Fig. 7. Experimental results showing slow speed reversal at nominal load torque: (a) original HF voltage signal and no models for inductance and flux variation; (b) modified HF voltage signal and models for inductance and flux variation. Explanations of the curves are as in Fig. 6.

$$
\begin{aligned}
\dot{\mathbf{i}}'_s = {} & \mathbf{L}^{-1}\mathbf{u}'_s - \tilde{\theta}_m\mathbf{L}^{-1}\mathbf{J}\mathbf{u}'_s + \tilde{\theta}_m\mathbf{J}\mathbf{L}^{-1}\mathbf{u}'_s \\
& -R_s\mathbf{L}^{-1}\mathbf{i}'_s + R_s\tilde{\theta}_m\mathbf{L}^{-1}\mathbf{J}\mathbf{i}'_s - R_s\tilde{\theta}_m\mathbf{J}\mathbf{L}^{-1}\mathbf{i}'_s \\
& +\tilde{\omega}_m\mathbf{J}\mathbf{i}'_s + 6\omega_m\mathbf{L}^{-1}\mathbf{J}\mathbf{L}_h\mathbf{i}'_s - 6\omega_m\tilde{\theta}_m\mathbf{L}^{-1}\mathbf{J}\mathbf{L}_h\mathbf{J}\mathbf{i}'_s \\
& +6\omega_m\tilde{\theta}_m\mathbf{J}\mathbf{L}^{-1}\mathbf{J}\mathbf{L}_h\mathbf{i}'_s - \omega_m\mathbf{L}^{-1}\mathbf{J}\mathbf{L}\mathbf{i}'_s \\
& +\omega_m\tilde{\theta}_m\mathbf{L}^{-1}\mathbf{J}\mathbf{L}\mathbf{J}\mathbf{i}'_s - \omega_m\tilde{\theta}_m\mathbf{J}\mathbf{L}^{-1}\mathbf{J}\mathbf{L}\mathbf{i}'_s \\
& -\mathbf{L}^{-1}\dot{\boldsymbol{\psi}}_{pm} - \tilde{\theta}_m\mathbf{J}\mathbf{L}^{-1}\dot{\boldsymbol{\psi}}_{pm} \\
& -\omega_m\mathbf{L}^{-1}\mathbf{J}\boldsymbol{\psi}_{pm} - \omega_m\tilde{\theta}_m\mathbf{J}\mathbf{L}^{-1}\mathbf{J}\boldsymbol{\psi}_{pm}
\end{aligned}
\tag{27}
$$

REFERENCES

[1] R. Wu and G. R. Slemon, "A permanent magnet motor drive without a shaft sensor," *IEEE Trans. Ind. Applicat.*, vol. 27, no. 5, pp. 1005–1011, Sept./Oct. 1991.

[2] R. B. Sepe and J. H. Lang, "Real-time observer-based (adaptive) control of a permanent-magnet synchronous motor without mechanical sensors," *IEEE Trans. Ind. Applicat.*, vol. 28, no. 6, pp. 1345–1352, Nov./Dec 1992.

[3] S. Bolognani, R. Oboe, and M. Zigliotto, "Sensorless full-digital PMSM drive with EKF estimation of speed and rotor position," *IEEE Trans. Ind. Electron.*, vol. 46, no. 1, pp. 184–191, Feb. 1999.

[4] M. Schroedl, "Sensorless control of AC machines at low speed and standstill based on the INFORM method," in *Conf. Rec. IEEE-IAS Annu. Meeting*, vol. 1, San Diego, CA, Oct. 1996, pp. 270–277.

[5] P. L. Jansen and R. D. Lorenz, "Transducerless position and velocity estimation in induction and salient AC machines," *IEEE Trans. Ind. Applicat.*, vol. 31, no. 2, pp. 240–247, March/April 1995.

[6] M. Linke, R. Kennel, and J. Holtz, "Sensorless position control of permanent magnet synchronous machines without limitation at zero speed," in *Proc. IEEE IECON'02*, vol. 1, Sevilla, Spain, Nov. 2002, pp. 674–679.

[7] E. Robeischl, M. Schroedl, and M. Krammer, "Position-sensorless biaxial position control with industrial PM motor drives based on INFORM and back EMF model," in *Proc. IEEE IECON'02*, vol. 1, Sevilla, Spain, Nov. 2002, pp. 668–673.

[8] M. Tursini, R. Petrella, and F. Parasiliti, "Sensorless control of an IPM synchronous motor for city-scooter applications," in *Conf. Rec. IEEE-IAS Annu. Meeting*, vol. 3, Salt Lake City, UT, Oct. 2003, pp. 1472–1479.

[9] A. Piippo, M. Hinkkanen, and J. Luomi, "Sensorless control of PMSM drives using a combination of voltage model and HF signal injection," in *Conf. Rec. IEEE-IAS Annu. Meeting*, vol. 2, Seattle, WA, Oct. 2004, pp. 964–970.

[10] A. Piippo and J. Luomi, "Adaptive observer combined with HF signal injection for sensorless control of PMSM drives," in *Proc. IEEE IEMDC'05*, San Antonio, TX, May 2005, pp. 674–681.

[11] T. S. Low, K. J. Tseng, T. H. Lee, K. W. Lim, and K. S. Lock, "Strategy for the instantaneous torque control of permanent-magnet brushless DC drives," *IEE Proc. B, Elect. Power Appl.*, vol. 137, no. 6, pp. 355–363, Nov. 1990.

[12] J. Holtz and L. Springob, "Identification and compensation of torque ripple in high-precision permanent magnet motor drives," *IEEE Trans. Ind. Electron.*, vol. 43, no. 2, pp. 309–320, Apr. 1996.

[13] M. W. Degner and R. D. Lorenz, "Using multiple saliencies for the estimation of flux, position, and velocity in AC machines," *IEEE Trans. Ind. Applicat.*, vol. 34, no. 5, pp. 1097–1104, Sept./Oct. 1998.

[14] J. Holtz, "Sensorless position control of induction motors—an emerging technology," *IEEE Trans. Ind. Electron.*, vol. 45, no. 6, pp. 840–852, Dec. 1998.

[15] N. Teske, G. M. Asher, M. Sumner, and K. J. Bradley, "Suppression of saturation saliency effects for the sensorless position control of induction motor drives under loaded conditions," *IEEE Trans. Ind. Electron.*, vol. 47, no. 5, pp. 1142–1150, Oct. 2000.

[16] A. Madani, J. Barbot, F. Colamartino, and D. Marchand, "An observer for the estimation of the inductance harmonics in a permanent-magnet synchronous machine," in *Proc. IEEE CCA'97*, Hartford, CT, Oct. 1997, pp. 517–521.

[17] A. Piippo, M. Hinkkanen, and J. Luomi, "Analysis of an adaptive observer for sensorless control of PMSM drives," in *Proc. IEEE IECON'05*, Raleigh, NC, Nov. 2005, pp. 1474–1479.

[18] T. Jahns, G. Kliman, and T. Neumann, "Interior permanent-magnet synchronous motors for adjustable-speed drives," *IEEE Trans. Ind. Applicat.*, vol. 22, no. 4, pp. 738–747, July/Aug. 1986.

[19] F. Briz del Blanco, M. W. Degner, and R. D. Lorenz, "Dynamic analysis of current regulators for AC motors using complex vectors," *IEEE Trans. Ind. Applicat.*, vol. 35, no. 6, pp. 1424–1432, Nov./Dec. 1999.

[20] J. K. Pedersen, F. Blaabjerg, J. W. Jensen, and P. Thogersen, "An ideal PWM-VSI inverter with feedforward and feedback compensation," in *Proc. EPE'93*, vol. 5, Brighton, UK, Sept. 1993, pp. 501–507.